Annealing effect on structural and electronic properties of iron-doped zinc oxide nanomaterials for theranostic application

Annealing effect on structural and electronic properties of iron-doped zinc oxide nanomaterials for theranostic application

Achmad Himawan[1,2]*, Ananta Agung Kurnia[1], Khusnul Hatimah Ilham[1], Dahlang Tahir[2], Muhammad Aswad[1], Abdur Rahman Arif[3]

[1]Faculty of Pharmacy, Universitas Hasanuddin, Makassar, Indonesia
[2]Physics Department, Faculty of Mathematics and Science, Universitas Hasanuddin, Makassar Indonesia
[3]Chemistry Department, Faculty of Mathematics and Science, Universitas Hasanuddin, Makassar Indonesia

*himawan@unhas.ac.id

Abstract. Zinc oxide has drawn attention to the development of theranostic material due to its superior biocompatibility compared to other semiconductor nanomaterials. Zinc oxide has a wide bandgap which favorable for quantum dots imaging agent. By coating zinc oxide with a suitable functional polymer, ZnO nanocrystal can be used for delivering the therapeutic agent and examining its effect on the biological environment. This research focuses on the comparison of ZnO and Fe-doped ZnO QDs characteristic synthesized from $ZnCl_2$ with co-precipitation method under the influence of different solvent and calcination temperature. The material was precipitated from solution by dropwise addition of sodium hydroxide solution in water and absolute ethanol. The resulting precipitate then calcined at 200, 400, 600 and 800°C for three hours. The materials then subjected to characterization process using UV-Vis spectroscopy and P-XRD. The results show that the ZnO and Fe-doped ZnO QD absorption spectra are redshifted toward the longer wavelength and the bandgap value analyzed using Tauc plot was smaller than the bulk bandgap of ZnO (3.37 eV).

1. Introduction

Zinc oxide nanocrystals is an interesting nanomaterial which has a wide range of application in the chemical, biomedical and pharmaceutical field [1], [2]. Both ZnO and diluted magnetic ZnO nanoparticles have a wide range direct band gap (3.37 eV) and large excitation binding energy (60 meV) and draw a lot of scientific interest [3], [4]. ZnO has good optical, electrical and chemical properties and widely used as a catalyst in the photochemical reaction and sensors. ZnO nanostructure also in the pharmaceutical and cosmetic industries for its antibacterial activity, anticancer activity, biosensor and drug carrier material [5], [6].

To improve physical characteristics of ZnO nanocrystal, adding metal ion dopant is one of the effective approaches. In doped ZnO, some Zn^{2+} ions are replaced with higher valency elements. By doping, structural, electrical and optical properties of ZnO nanomaterials can be enhanced [7]. Fe doping of ZnO results in different emission spectra and different nanostructure. Doping with Fe can prevent recombination of the photo-generated electron-hole pair which leads to the improvement of

photocatalytic activities of ZnO nanocrystal [8]. The previous study had found that annealing temperature affects the crystal and particle size of ZnO nanoparticles synthesized via sol-gel technique. This study found that the crystal and particle size were enlarged alongside the calcination temperature increment [5]. Another study showed that the crystalline size of ZnO is decreasing with the addition of Fe as a dopant element [3].

A water-stable material and, in some case, clear emission in the visible range are required for most bioanalysis purposes [9], which includes core material for a theranostic material which is aimed at this research. In this research, we report the effect of solvent and annealing temperature in the characteristic of Fe-doped ZnO for theranostic purposes. The ZnO is synthesized using a simple solution method to produce water stable Fe-doped ZnO from $ZnCl_2$ and $FeCl_3$.

2. Experimental

2.1. Materials

Zinc chloride anhydrate, ferric chloride anhydrate, sodium hydroxide, and methylene blue were obtained from Merck Chemical Company, while absolute ethanol was acquired from J.T. Baker. Deionized water was acquired from Ika-Pharmindo. All chemicals were used without further purification.

2.2. Preparation of Undoped ZnO Nanocrystal and Fe^{3+}-Doped ZnO Nanocrystal

The ZnO nanocrystals were prepared using the coprecipitation method using zinc chloride as the precursors. Two different solvents were used in this study, which is deionized water and absolute ethanol. 50 ml of Zinc chloride solution 0,035 M was prepared by mixing zinc chloride with a solvent in an Erlenmeyer flask until complete dissolution. The mixture then heated to 65 ± 5 °C and vigorously stirred using a magnetic stirrer for 30 min at 65 ± 5 °C under reflux condition. The resulting mixture then cooled in the fridge until it reached room temperature. The same volume of sodium hydroxide solution 0,070 M also prepared using the same solvent. Sodium hydroxide solution was added dropwise to zinc chloride solution under vigorous stirring with a magnetic stirrer. The mixture then centrifuged at 3000 rpm to collect all the precipitate. The precipitate then washed three times with absolute ethanol before dried at 80 °C for three hours. The dried mass then calcined at 200, 400, 600 and 800 °C for 3 hours. Fe^{3+}-doped ZnO nanocrystals were prepared with the same method with the addition of 1 ml ferric chloride solution containing 0.5% wt. Fe prior base addition.

2.3. Characterization

2.3.1. Optical Properties Analysis.

The UV-Visible absorption spectrum of ZnO and Fe3+-doped ZnO was recorded using Shimadzu UV-Vis Spectrophotometer from 200 to 800 nm. The absorption data then used to calculate the direct bandgap using Tauc Plot based on Eq. (1)

$$\alpha h\nu = E_d\left(h\nu - E_g\right)^{1/2} \quad (1)$$

2.3.2. X-Ray Diffraction Analysis.

ZnO and Fe^{3+}-doped ZnO were analyzed using Powder X-Ray Diffractometer to determine its crystal phase composition and crystal size. The sample was scanned from 25 to 75° with a scanning speed of 2°/min. CuKα (40 kV, 30 mA) was used as the radiation source. The average crystal size was determined based on the Scherrer method using Eq. (2) and the lattice parameter was determined using Eq (3-9).

$$D = \frac{0.9\lambda}{\beta \cos\theta} \quad (2)$$

$$\delta = \frac{1}{D^2} \tag{3}$$

$$\varepsilon = \frac{\beta}{4\tan\theta} \tag{4}$$

$$\frac{1}{d^2} = \frac{4}{3}\frac{(h^2 + hk + k^2)}{a^2} + \frac{l^2}{c^2} \tag{5}$$

$$V = \frac{\sqrt{3}}{2}a^2c \tag{6}$$

$$u = \frac{a^2}{3c^2} + 0.25 \tag{7}$$

$$L = \sqrt{0.3a^2 + (0.5 - u)^2c^2} \tag{8}$$

$$APF(\%) = \frac{2\pi a}{3\sqrt{3}c^2} \times 100 \tag{9}$$

3. Results and Discussion

The nanocrystal was synthesized using precipitation method form $ZnCl_2$ starting materials. The reaction for zinc oxide formation can be written as:

$$ZnCl_2 + 2\ NaOH \rightarrow ZnO + 2\ NaCl + H_2O$$

and for Fe3+-doped zinc oxide, the reaction can be simplified and written as:

$$ZnCl_2 + 2\ NaOH + Fe^{3+} \rightarrow Zn_{99.5}Fe_{0.5}O + 2\ NaCl + H_2O$$

UV-Visible spectra of the ZnO and Fe^{3+}-doped ZnO is shown in Figure 1-4 and calculate bandgap, as well as the maximum absorption wavelength, are shown in Table 1. Bandgap lowering effect by dopant addition has been observed before and can be explained by the s-d and p-d exchange interaction between the band electron in ZnO and localized electron in Fe^{3+}. The direct bandgap value was decreased as the temperature increase while the λ_{max} of the absorption spectra were red-shifted due to different crystalline size resulted from different annealing temperature. The λ_{max} shifting, caused by the dopant addition and indicate the incorporation of Fe^{3+} ion in ZnO crystal lattice. The reported results agreed with a similar study reported previously [5], [8], [10]. The calculated bandgap of Fe^{3+}-doped ZnO precipitated from water and calcined at 800°C fall below three which is out of the usable range for the most application of ZnO nanoparticles [5]. However, this value was smaller than the known bulk bandgap of the ZnO. The relationship between annealing temperature and energy bandgap is shown in Figure 5.

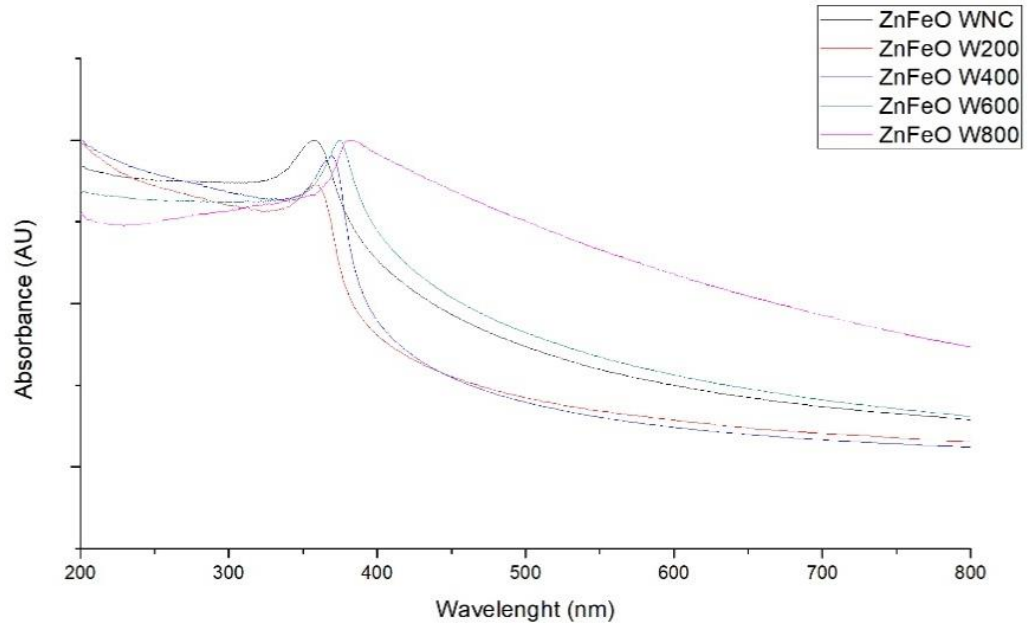

Figure 1. UV-Vis spectra of Fe^{3+}-doped ZnO nanocrystal prepared with water

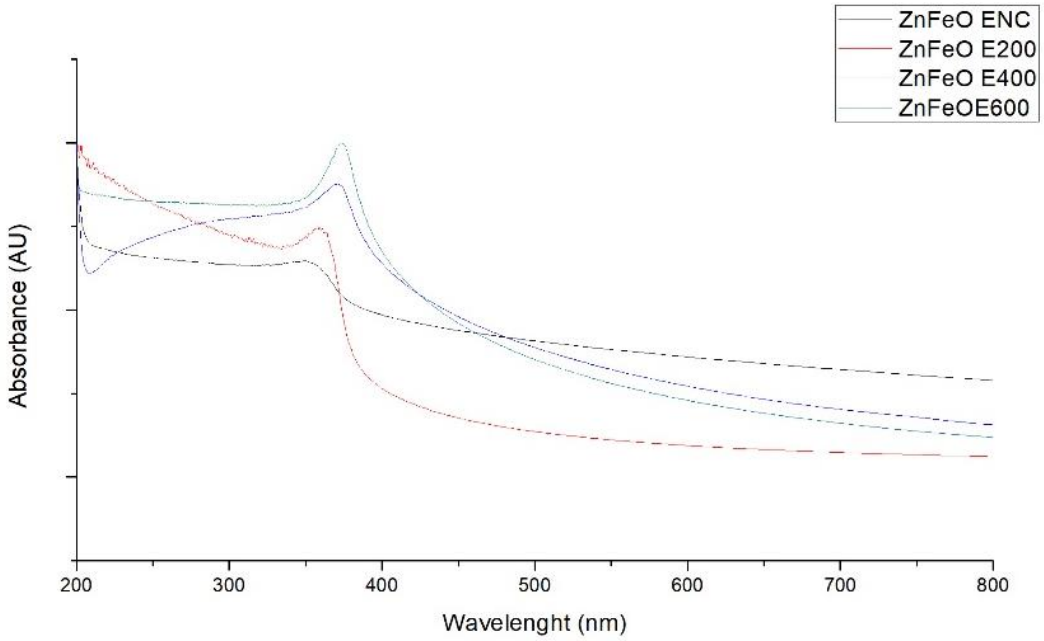

Figure 2. UV-Vis spectra of Fe^{3+}-doped ZnO nanocrystal prepared with ethanol

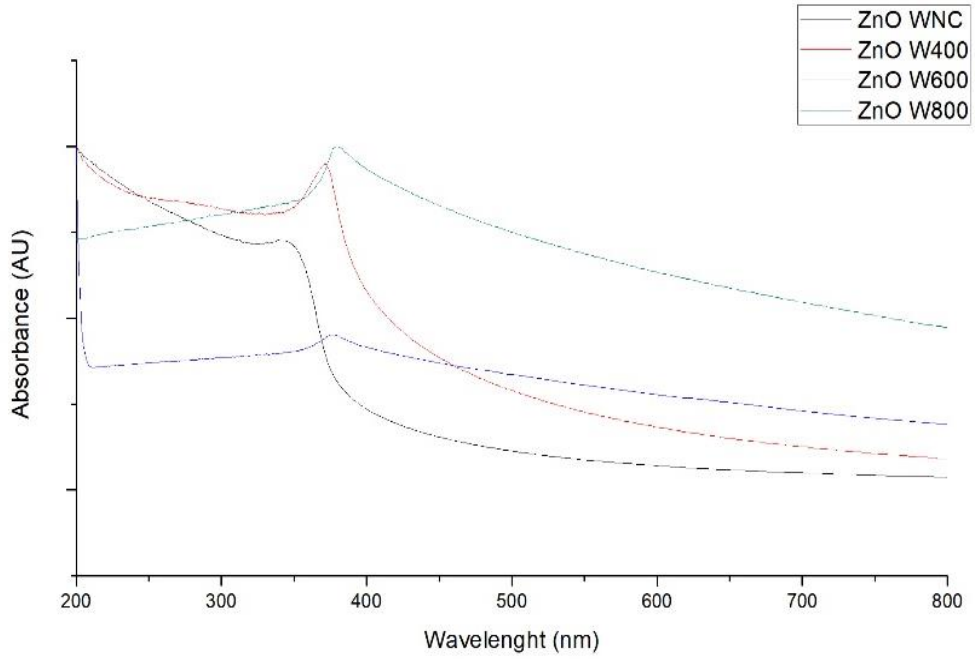

Figure 3. UV-Vis spectra of undoped ZnO nanocrystal prepared with water

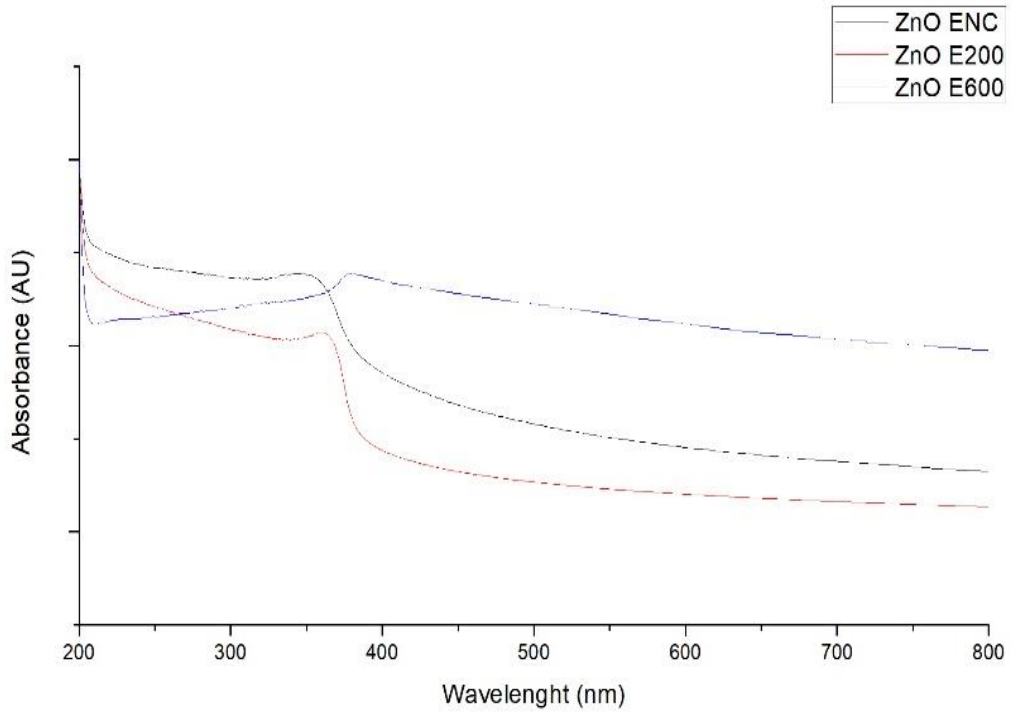

Figure 4. UV-Vis spectra of undoped ZnO nanocrystal prepared with ethanol

Table 1. Energy Bandgap of ZnO and Fe^{3+}-doped ZnO

Sample	Solvent	Annealing Temp	Maximum Absorption Wavelength	Energy Gap
Undoped ZnO	Ethanol	NC	342.o nm	3.05 eV
		200	358.5 nm	3.24 eV
		400	NA	NA
		600	381.0 nm	2.12 eV
		800	NA	NA
	Water	NC	340.0 nm	3.22 eV
		200	NA	NA
		400	372.0 nm	3.02 eV
		600	377.0 nm	2.62 eV
		800	379.5 nm	2.45 eV
Fe^{3+}-doped ZnO	Ethanol	NC	350.0 nm	3.01 eV
		200	361.5 nm	3.20 eV
		400	371.0 nm	3.07 eV
		600	374.5 nm	3.04 eV
		800	NA	NA
	Water	NC	357.5 nm	3.03 eV
		200	359.5 nm	3.17 eV
		400	370.0 nm	3.13 eV
		600	374.5 nm	3.00 eV
		800	381.5 nm	2.33 eV

NC: Not Calcined
NA: Not Applicable

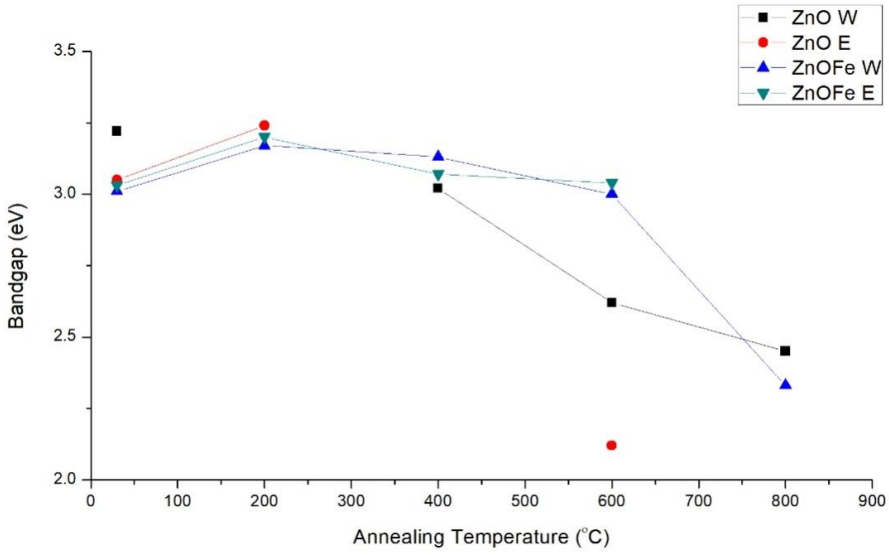

Figure 5. Relationship Between Annealing Temperature and Energy Bandgap of Undoped and Fe^{3+}-doped ZnO Nanocrystal

The X-Ray diffractogram of undoped and doped ZnO was shown in Figure 6. The figure reveals peaks that correspond to (100), (002), (101), (012), (110), (013), and (112) planes related to the hexagonal structure of wurtzite form of ZnO. The Fe^{3+} dopant and solvent usage do not affect the major peaks to the corresponding ZnO crystal plane, which implies that there is no deformation on the structure of the nanocrystal. The sharpened peaks of Fe^{3}-doped ZnO nanoparticles (prepared both in water and ethanol) after calcination at various temperature indicate crystal growth at a higher temperature and better crystallinity [5], [7], [11]. Figure 7 shows a zoomed picture of three major peaks from the materials, and it shows how the peak is slightly shifted due to the solvent effect, and this indicates the increase of the lattice parameter.

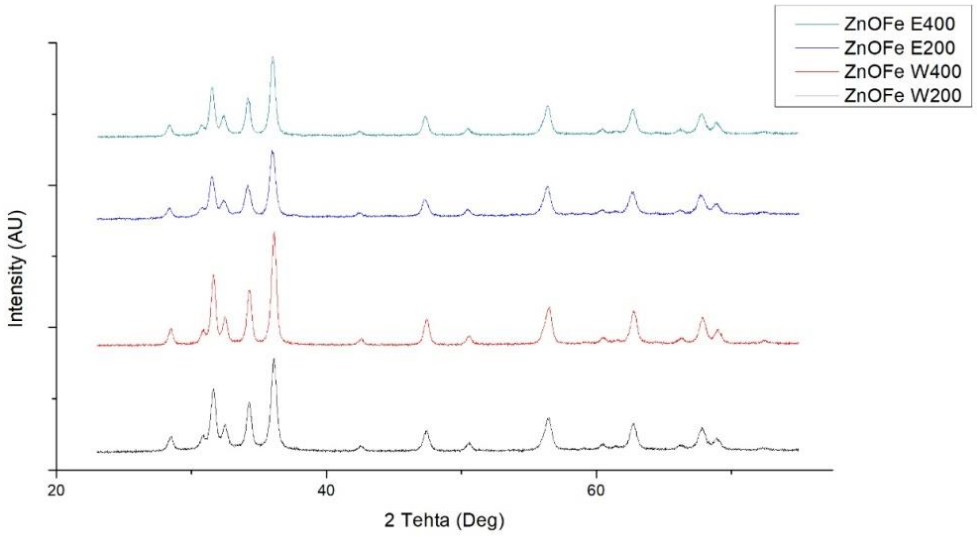

Figure 6. PXRD Profile

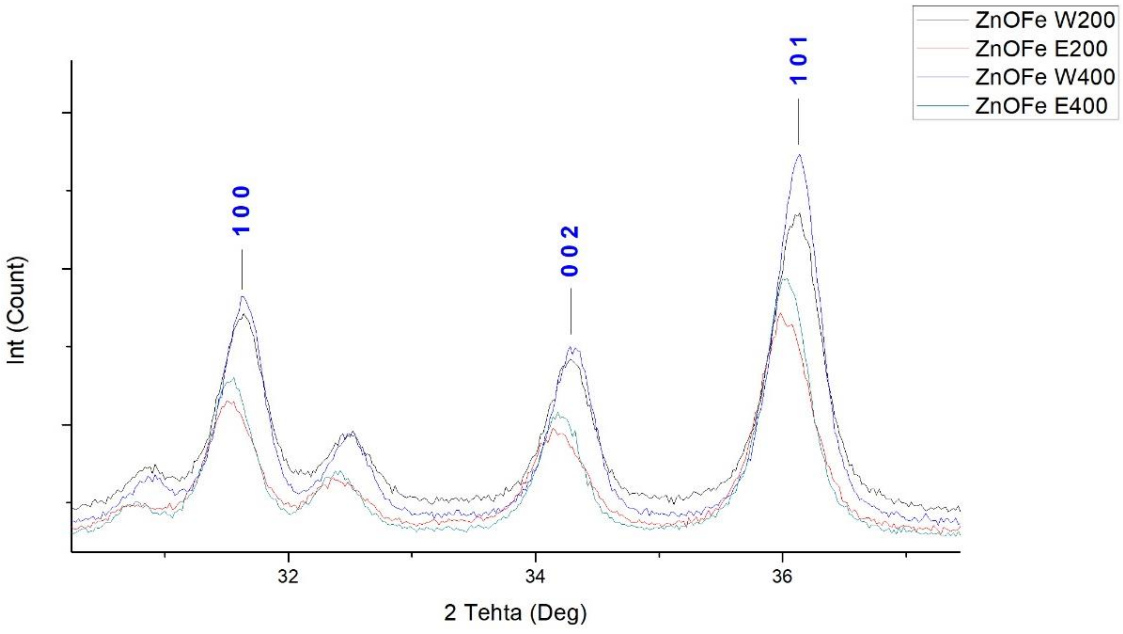

Figure 7. Observed Peak Shift in PXRD Profile

The structural and lattice parameter calculation was done based on PXRD data on Fe^{3+}-doped ZnO. The evaluated grain size (D) of the particles varies from 16.12-18.73 nm Similar finding of the growth of crystal had been reported and in a complete agreement of the sharpened diffraction peak [12]. Materials synthesized using water as the solvent has a larger average size compared to the one produced using ethanol. It is suggested that interaction between solvent and precipitate may play a role in controlling the crystalline size of the produced materials. The dislocation density corresponds to defect present in particles during deposition. Higher annealing temperature results in the decreasing dislocation density value thus imply on less defect at higher calcination temperature. The lattice strain was also found to be minimum at the higher annealing temperature.

Table 2. Structural Parameter of Fe^{3+}-doped ZnO Nanocrystal

Sample	Solvent	Annealing Temp	Grain Size* ($D_{average}$)	Lattice Strain (ε) ($x10^{-3}$)	Dislocation Density (δ) ($x10^{15}$)
Fe^{3+}-doped ZnO	Ethanol	200	16.12 nm	6.90	3.85
		400	18.40 nm	5.98	2.95
	Water	200	17.08 nm	6.41	3.43
		400	18.73 nm	5.72	2.85

*$D_{average}$ is calculated using eight strongest peaks of the sample

The lattice parameter and unit cell volume were calculated using a well-known method for the hexagonal lattice system. The results show that the calculated *a* and *c* are slightly larger than of the known value for ZnO in the literature due to the difference between Zn^{2+} and Fe^{3+} radii (a = 3.249 Å and c = 5.205 Å) [10], [13], [14]. Unit cell volume (*V*), the internal parameter (*u*), bond length (*L*) and atomic packing factor (APF) are presented in Table 3. A very subtle change was observed in all calculated value due to varying lattice parameter. Increasing unit cell volume after the addition of 0.5% wt of Fe reported by a similar study which caused by increasing lattice parameter (*a* and *c*) value) [15]. This study report that by increasing the temperature from 200 to 400°C, in both water and ethanol-mediated synthesis, the lattice parameters *a* was elongated while c was shortened and affect the other calculated value. The bond length in the crystalline structure was slightly longer when using ethanol as the solvent. The increasing of lattice parameters was in the good agreement with increasing crystalline size. The increasing u parameter and decreasing c/a parameter (Figure 9) indicate the slight alteration of the four-tetrahedral distance within the lattice resulting from the different solvent and annealing temperature.

Table 3. Lattice Parameter from corresponding main peak

Sample	Solvent	Annealing Temp	Crystal Plane	*d* (Å)	*a* (Å)	*c* (Å)	*c/a*	*V* ($Å^3$)	*u*	*L* (Å)	APF (%)
Fe-doped ZnO	Ethanol	200	101	2.4935	3.2761	5.2260	1.5951	48.57	0.3810	1.899	75.76%
		400	101	2.4942	3.2782	5.2218	1.5929	48.60	0.3813	1.899	75.87%
	Water	200	101	2.4874	3.2669	5.2210	1.5982	48.25	0.3805	1.895	75.62%
		400	101	2.4881	3.2681	5.2205	1.5974	48.29	0.3806	1.895	75.66%

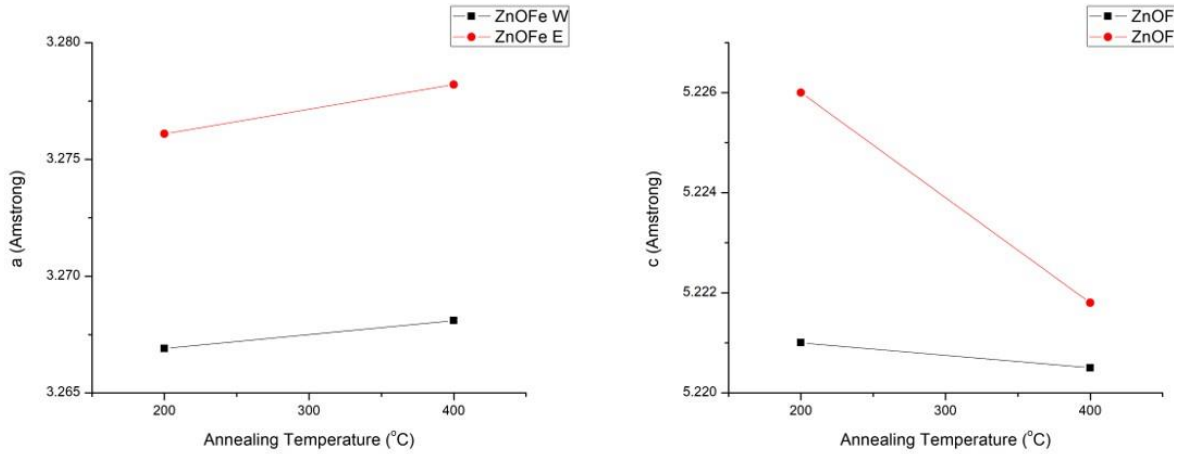

Figure 8. Change in lattice parameters a and c vs annealing temperature

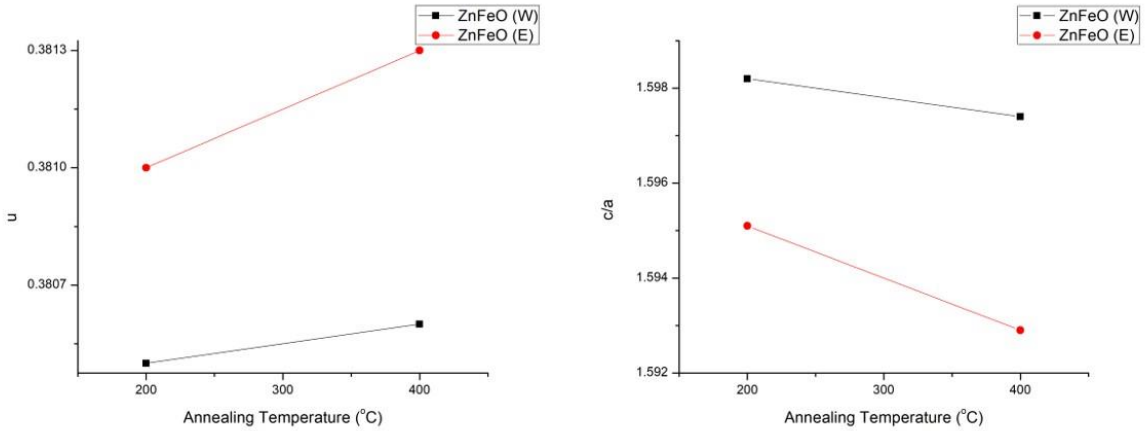

Figure 9. Change in lattice parameters u and c/a vs annealing temperature

4. Conclusion

Annealing temperature affects the optical of undoped and Fe3+-doped ZnO to a certain extent. Increasing annealing temperature decrease the bandgap and for some treatment, fall below the desired value for the theranostic application. The lattice parameter in Fe3+-doped ZnO nanocrystals is slightly different after treatment with different annealing temperature. The crystalline size, crystallinity, a. and u increases as the calcination increased from 200 to 600°C while lattice strain, dislocation density, c and c/a parameter is decreased. In this research, we conclude that for annealing temperature and solvent usage, using water and calcination at 200°C is the optimum parameter to produce Fe3+-doped ZnO with precipitation method from ZnCl2.

Acknowledgment

The authors are thankful to the Universitas Hasanuddin for their financial support. Part of this research was funded by Universitas Hasanuddin via “Penelitian Dosen Pemula” Research Grant.

References

[1] V. Mușat, M. B. Ibănescu, D. Tutunaru, and F. Potecaşu, “Fe-Doped ZnO Nanoparticles : Structural , Morphological , Antimicrobial and Photocatalytic Characterization,” vol. 1143, pp. 233–239, 2017.

[2] Q. Yuan, S. Hein, and R. D. K. Misra, “New generation of chitosan-encapsulated ZnO quantum

dots loaded with drug: Synthesis, characterization and in vitro drug delivery response," *Acta Biomater.*, vol. 6, no. 7, pp. 2732–2739, 2010.

[3] R. Ashraf, S. Riaz, Z. Nazir, and S. Naseem, *Structural and magnetic properties of iron doped ZnO nanoparticles*, vol. 2, no. 10. Elsevier Ltd., 2015.

[4] M. M. Ba-abbad, A. Amir, H. Kadhum, A. Bakar, and M. S. Takriff, "Visible Light Photocatalytic Activity of Fe3+ -doped ZnO Nanoparticle Prepared via Sol–Gel Technique," *Chemosphere*, 2013.

[5] M. M. Ba-abbad, A. Amir, H. Kadhum, A. Bakar, and M. S. Takriff, "The effect of process parameters on the size of ZnO nanoparticles synthesized via the sol – gel technique," *J. Alloys Compd.*, vol. 550, pp. 63–70, 2013.

[6] H. Mirzaei and M. Darroudi, "Zinc oxide nanoparticles_ Biological synthesis and biomedical applications," *Ceram. Int.*, vol. 43, no. 1, pp. 907–914, 2017.

[7] T. Srinivasulu, K. Saritha, and K. T. R. Reddy, "Synthesis and characterization of Fe-doped ZnO thin fi lms deposited by chemical spray pyrolysis," *Mod. Electron. Mater.*, vol. 3, no. 2, pp. 76–85, 2017.

[8] X. Yu, D. Meng, and C. Liu, "Enhanced photocatalytic activity of Fe-doped ZnO nanoparticles synthesized via a two-step sol – gel method," pp. 1–4, 2014.

[9] M. K. Patra *et al.*, "Synthesis of stable dispersion of ZnO quantum dots in aqueous medium showing visible emission from bluish green to yellow," *J. Lumin.*, vol. 129, no. 2009, pp. 320–324, 2009.

[10] S. Kanchana, M. J. Chithra, S. Ernest, and K. Pushpanathan, "Violet emission from Fe doped ZnO nanoparticles synthesized by precipitation method," *J. Lumin.*, vol. 176, pp. 6–14, 2016.

[11] J. Z. Kong *et al.*, "Photo-degradation of methylene blue using Ta-doped ZnO nanoparticle," *J. Solid State Chem.*, vol. 183, no. 6, pp. 1359–1364, 2010.

[12] A. K. Zak, M. E. Abrishami, W. H. A. Majid, R. Yousefi, and S. M. Hosseini, "Effects of annealing temperature on some structural and optical properties of ZnO nanoparticles prepared by a modified sol-gel combustion method," *Ceram. Int.*, vol. 37, no. 1, pp. 393–398, 2011.

[13] "Structural and dielectric properties of Fe doped ZnO nanoparticles Structural and dielectric properties of Fe doped ZnO nanoparticles," no. June 2014, 2012.

[14] O. D. Jayakumar, H. G. Salunke, R. M. Kadam, M. Mohapatra, G. Yaswant, and S. K. Kulshreshtha, "Magnetism in Mn-doped ZnO nanoparticles prepared by a co-precipitation method," *Nanotechnology*, vol. 17, no. 5, pp. 1278–1285, 2006.

[15] A. Thurber *et al.*, "Improving the selective cancer killing ability of ZnO nanoparticles using Fe doping," vol. 6, no. June, pp. 440–452, 2012.